Carbon monoxide hydrogenation over Fe/HZSM-5 catalysts. Effect of SiO_2/Al_2O_3 zeolite ratio

G. Calleja [1], A. de Lucas, R. van Grieken, J.L. Peña
Department of Chemical Engineering, Universidad Complutense, 28040 Madrid, Spain

A. Guerrero-Ruiz
Department of Inorganic Chemistry, UNED, 28028 Madrid, Spain

and

J.L.G. Fierro
Institute of Catalysis and Petrochemistry, CSIC, Campus UAM, Cantoblanco, 28049 Madrid, Spain

Received 14 September 1992; accepted 8 December 1992

Iron catalysts supported on ZSM-5 zeolites of a wide range of silica-to-alumina ratios (29–∞) have been prepared and tested in carbon monoxide hydrogenation. The crystalline phases of the catalysts were characterized by X-ray diffraction and their acidity by infrared spectroscopy of adsorbed pyridine. The catalytic tests were conducted at 533 K, an overall pressure of 21 bar and a feed ratio CO/H_2 close to 1. It was found that the selectivity to light olefins (C_2–C_4) increases in parallel with the increase of the Si/Al ratio of the zeolite. This was explained in terms of the decrease in Brønsted acidity of the catalysts. As a consequence, very high olefin selectivities can be achieved by decreasing the number of strong acid sites in the zeolite structure, but at the expense of high oxygenate formation.

Keywords: Fe/HZSM-5 zeolite catalysts; carbon monoxide hydrogenation; infrared spectra of chemisorbed pyridine; X-ray diffraction

1. Introduction

The production of liquid hydrocarbons from synthesis gas (CO/H_2) via Fischer–Tropsch (FT) processes is a promising, developing option for the production of clean fuels and chemicals from natural gas or coal. Much of the developments on FT synthesis took place in Germany during the 1930's and 40's, which then led to the commissioning of the Sasol plant in South Africa, the only large scale commercial operation. There is indeed a vast body of work on this subject, but

---

[1] To whom correspondence should be addressed.

most of the details and developments on FT catalysts and processes can be found in a grouped manner in excellent reviews [1,2].

As is well known, one of the most important limitations of FT is selectivity. This is due to the fact that the chain growth mechanism for FT synthesis is governed by Anderson–Schulz–Flory (ASF) kinetics [3]. While product molecular weight can be modified by an appropriate selection of the catalyst and the process conditions to obtain a given degree of polymerization, a wide hydrocarbon distribution is inherent. Apart from this, the conversion of synthesis gas into hydrocarbon mixtures on FT catalysts has progressed considerably in recent years in attempting to avoid the intrinsic limitations in selectivity of the conventional processes [4]. The selective production of low molecular weight olefins (C_2–C_4) is one of the most interesting alternatives to the carbon monoxide hydrogenation to liquid hydrocarbons with the classical FT process [5,6]. To achieve this objective, the combination of shape-selective zeolites (ZSM-5 and silicalite) with first-row transition metal FT catalysts appears to be very attractive [7–9]. The activity, stability and selectivity of this kind of catalyst may be significantly affected by the physicochemical properties of the zeolite substrate. A change in the aluminium content of the zeolite produces differences in the number and distribution of acid sites, which induces sharp changes in the catalytic activity, ion-exchange capacity and hydrophobic properties of the zeolite.

As there is very limited information on the influence of the gradual changes of the acidity of zeolite substrate for FT synthesis [8], this work reports catalytic behavior of several iron catalysts supported on HZSM-5 zeolites of a wide range of silica-to-alumina ratios. As these zeolites have the same structure, the differences in catalytic performance can be related to the acidity changes of these substrates.

2. Experimental

2.1. CATALYST PREPARATION

Three proton-exchanged ZSM-5 zeolites with SiO_2/Al_2O_3 ratios of 29, 56 and 88, and a silicalite-1 zeolite ($SiO_2/Al_2O_3 = \infty$) were synthesized following the experimental procedure described in ref. [10]. The SiO_2/Al_2O_3 ratios were determined following the procedure of Hillebrand et al. [11]. The total Al was determined by measuring this element in the filtrate from the evaporation following HF and H_2SO_4 treatments. The residue was fused with Na_2CO_3 and brought into solution before measurement by atomic absorption.

The iron-zeolites were prepared by impregnating the zeolite with aqueous solutions of $Fe(NO_3)_3 \cdot 9H_2O$ (Merck, reagent grade) in appropriate amounts so as to yield iron concentrations close to 8 wt%. The impregnates were dried at 383 K for 12 h and then calcined at 823 K for 5 h.

2.2. CATALYST CHARACTERIZATION

The examination of the surface acidity of the unreduced catalysts was carried out by infrared spectroscopy of adsorbed pyridine. Very thin self-supporting wafers ($\approx$ 8 mg cm^{-2}) of the calcined samples were placed in a special infrared cell, assembled with greaseless stopcocks and KBr windows. The samples were first outgassed in high vacuum at 723 K for 4 H and then cooled down to room temperature prior to exposure to about 3 Torr (1 Torr = 133.33 N m^{-2}) pyridine. The physically adsorbed pyridine was removed by outgassing at 393 K for 0.5 h. The spectra were recorded using a Nicolet 5ZDX Fourier Transform spectrophotometer at a resolution of 4 cm^{-1}.

The X-ray diffraction measurements were made using a Siemens Kristalloflex D500 diffractometer equipped with a copper X-ray tube operated at 40 kV and 20 mA, a nickel filter and a graphite receiving monochromator. The scans for the calcined, reduced and activated catalysts were made over the range 5–65 2Θ at 0.02° intervals. Tungsten powder was used as an internal standard for the correction of the angles and of the instrumental broadening for crystal size measurement. The crystal phase composition of the samples were determined by comparison with standard ASTM files.

2.3. ACTIVITY MEASUREMENTS

The catalysts were tested in a continuous flow system with a single pass, fixed bed downflow reactor. Feed gases were H_2 (99.995 vol%, Argon Co.) and CO (99.97 vol%, Matheson Co.), measured by means of Brooks mass flow controllers. Details regarding this configuration can be found elsewhere [12]. The reaction conditions selected for the catalyst tests were: reaction temperature 533 K, overall pressure 21 bar, molar ratio in the feed $H_2/CO = 1$, and WHSV = 2 h^{-1}. The catalysts were reduced in situ at 673 K for 12 h with a mixture of 20% H_2 in He. Then the temperature was set at 423 K and the H_2/CO mixture admitted at 1 bar; subsequently temperature increased slowly up to 533 K and pressure up to 21 bar. These conditions were maintained for 12 h on-stream to reach steady state conditions. Reactants and products were analyzed by gas chromatography. The exiting gases were passed through a Porapak Q column for separation, and then analyzed by TCD. The condensate was decanted, alcohols and hydrocarbons being then separated in a Porapak Q column connected to a TCD and a capillary column connected to a FID.

3. Results and discussion

Activity results under the specific reaction conditions used showed that the CO conversion remains essentially constant ($\approx$ 4%) for all Fe-loaded zeolite catalysts irrespective of the SiO_2/Al_2O_3 ratio of the zeolite substrate. However, the product distribution was strongly influenced by this ratio as shown in fig. 1a for carbon dioxide, hydrocarbons and alcohols, and in fig. 1b for the different hydrocarbon fractions, including methane, olefins, paraffins and longer hydrocarbons (C_{5+}).

From the results in figs. 1a and 1b it is clear that the less acidic Fe/silicalite-1 catalyst displays a moderately high ($\approx$ 50%) selectivity to carbon dioxide. All catalysts show a low selectivity ($\approx$ 5%) to low molecular weight saturated alcohols, and selectivity decreases upon increasing acidity of the zeolite substrate. This fact may be related to the capability of the acid sites of the zeolite to dehydrate alcohols and polymerise the resulting olefins into longer chain hydrocarbons by a mechanism similar to that involved in the MTG of Mobil. Owing to the reducing environment of the catalyst during operation, carbon dioxide should not be expected

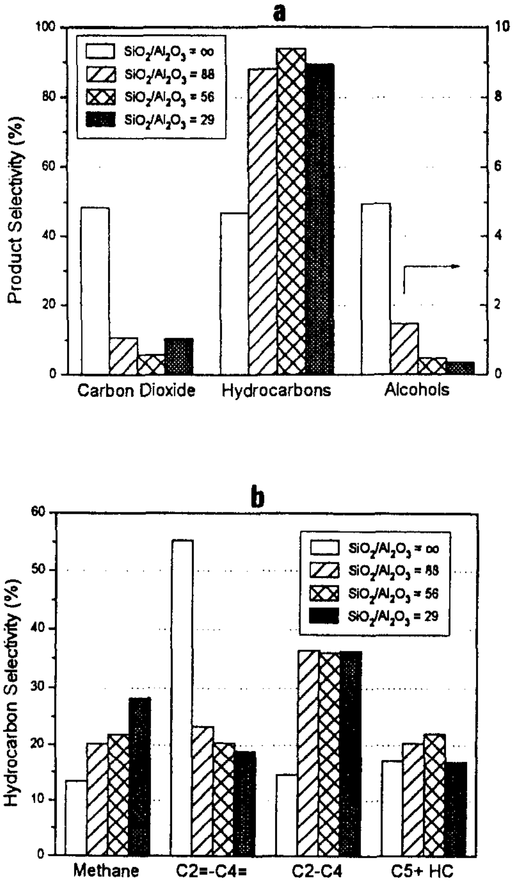

Fig. 1. Selectivity changes to the reaction products carbon dioxide, hydrocarbons and low molecular weight saturated alcohols (a), and hydrocarbon distribution (b) as a function of the silica-to-alumina ratio of Fe/ZSM-5 catalysts.

from the direct hydrogenation reaction. However, it can be formed to a certain extent through the undesired and simultaneous water–gas shift ($CO + H_2O \rightarrow CO_2 + H_2$), and perhaps CO disproportionation ($2CO \rightarrow C + CO_2$), reaction. It can also be noted in the hydrocarbons fraction a moderately high ($\approx 56\%$) selectivity to low molecular weight (C_2–C_3) olefins, which is accompanied by a low selectivity to methane and paraffins.

Upon decreasing the SiO_2/Al_2O_3 ratio of the zeolite from 88 to 29 the proportion of both oxygenated compounds and light olefins also decreases. Simultaneously, the yield to saturated hydrocarbons, including methane, light paraffins and hydrocarbons with more than five C-atoms, is improved. It can also be noted that for the Fe/ZSM-5 ($SiO_2/Al_2O_3 = 29$) catalyst the CO_2 selectivity is slightly higher than for the other two less acidic Fe/ZSM-5 catalysts. This phenomenon may be explained in terms of the greater participation of coke deposition resulting from the higher olefinic fraction on this catalyst, since the zeolite substrate is the most acidic of the series. Coke deposition is the last step of a complex mechanism involving dehydrogenation and condensation reactions [13]. This hypothesis is strengthened by the X-ray diffraction pattern of the spent catalyst, which showed a single diffraction line between Bragg's angles of 44° and 46°, whereas the fresh Fe/ZSM-5 homologue catalyst displays the characteristic doublet in the same diffraction angle region. The disappearance of the doublet was interpreted by Pollack et al. [14] as due to a decrease in the *a* axis which decreases by about 0.005 nm while the *b* axis increases by about 0.005 nm, and proposed the filling of the pores of the zeolite or the changes of the SiO_2/Al_2O_3 ratio as possible causes of these shifts. As no dealumination is expected to occur under the experimental conditions used in this work we believe that the broad single diffraction line is due to filling of the zeolite pores.

The X-ray diffraction technique was very useful in the identification of the iron phases at different steps of the genesis of catalysts. For the calcined catalysts only the α-Fe_2O_3 was observed, whereas the α-Fe phase and a χ-Fe_5C_2 iron carbide (and perhaps a very small amount of ε-$Fe_{2.2}C$) were found respectively in the H_2-reduced catalysts and catalysts activated in the reaction mixture ($H_2 : CO = 1$).

The infrared spectra in the spectral region 1700–1400 cm^{-1} of adsorbed pyridine on calcined and outgassed catalysts are shown in fig. 2. With the exception of the Fe/silicalite-1, the other three Fe/ZSM-5 catalysts (spectra b–d) show typical bands of adsorbed pyridine at about 1450, 1490, 1540 and 1620 cm^{-1}. The bands at about 1450 and 1540 cm^{-1} are usually attributed to the stretching vibration of pyridine coordinated to Lewis acid sites and to the stretching vibration mode of C–C bonds in the pyridinium ion (PyH^+), respectively, the latter being frequently used to detect and quantify Brønsted acid sites [15–18]. The other two bands at about 1490 (very strong) and 1620 (weak) cm^{-1} contain contributions of the two types of acidity. It is clear from fig. 2 that the intensity of the band at about 1450 cm^{-1} increases, as expected, with the aluminum content of the zeolite, which corre-

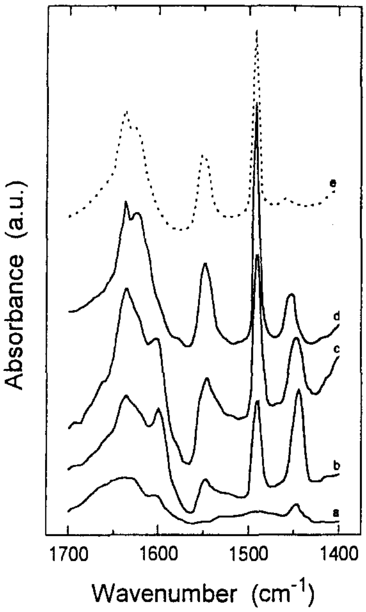

Fig. 2. Infrared spectra of adsorbed pyridine on calcined and outgassed Fe/ZSM-5 zeolite catalysts with silica-to-alumina ratios of: ∞ (a); 88 (b); 56 (c); 29 (d). For comparative purpose the spectrum of pyridine adsorbed on the original ZSM-5 zeolite ($SiO_2/Al_2O_3 = 56$) is also included (e).

sponds to the increasing Brønsted acidity of the catalysts. For the Fe/silicalite-1 catalyst the absence of aluminum in the substrate silicalite-1 zeolite can explain the failure to detect Brønsted acidity and the observation of weak Lewis acidity due to the Fe_2O_3 phase. Consistent with these results, potentiometric titration measurements revealed the presence of a small proportion of weak Lewis sites in this catalyst.

The comparison of the acidity data with the product distribution indicates that there is a close parallel between the decrease in selectivity toward oxygenates and low molecular weight olefins and the increase in Brønsted acidity of the Fe/zeolite catalysts. The opposite trend found for methanation, and particularly for the most acid catalyst ($SiO_2/Al_2O_3 = 29$), suggests that the most acid catalyst possess a higher capability for CO hydrogenation, yielding methane as the major product. Similarly, as Brønsted acidity promotes chain growth via carbocations, the hydrocarbon C_{5+} fraction increases for the Fe/ZSM-5 ($SiO_2/Al_2O_3 = 56$) catalyst with respect to its Fe/ZSM-5 ($SiO_2/Al_2O_3 = 88$) homologue. By contrast, the lower C_{5+} hydrocarbon product from the most acid catalyst ($SiO_2/Al_2O_3 = 29$) is unexpected. The explanation of this unusual behaviour may lie in the strong deactivation of this zeolite.

4. Conclusion

Iron-loaded silicalite-1 (SiO_2/Al_2O_3 ratio $= \infty$) and H-ZSM-5 zeolites (SiO_2/Al_2O_3 ratios $= 29$, 56 and 88) have been used in the CO hydrogenation reaction. Although activity is similar for all catalysts, the product distribution markedly depends on the acidity of the substrate zeolite. In particular, the Fe/silicalite-1 catalyst with no acid sites displays a quite dissimilar product distribution. Also, the most acidic Fe/ZSM-5 ($SiO_2/Al_2O_3 = 29$) catalyst shows a strong deactivation due to coke formation. On comparing the infrared spectra of chemisorbed pyridine (fig. 2) and the product distribution a relationship between the decrease in oxygenates selectivity and low molecular weight olefins and the increase of Brønsted acidity of catalyst is evident.

Acknowledgement

This research was supported by the CICYT (Spain) (Grant MAT 91-0494). One of us (JLP) thanks the Ministry of Education and Science for a fellowship.

References

[1] M.E. Dry, in: *Catalysis Science and Technology*, eds. J.R. Anderson and M. Boudart (Springer, Berlin, 1981) pp. 159–256.
[2] R.B. Anderson, *The Fischer–Tropsch Synthesis* (Academic Press, New York, 1984).
[3] D.L. King, J.A. Cusumano and R.L. Garten, Catal. Rev.-Sci. Eng. 23 (1981) 233.
[4] C.H. Bartholomew, Catal. Lett. 7 (1990) 303.
[5] R. Snell, Catal. Rev.-Sci. Eng. 29 (1987) 361.
[6] M. Janardanarao, Ind. Eng. Chem. Res. 29 (1990) 1735.
[7] V.U.S. Rao and R.J. Gormley, Hydroc. Process. 11 (1980) 139.
[8] F.G. Dwyer and W.E. Garwood, *Catalytic Conversions of Synthesis Gas and Alcohols to Chemicals* (Plenum Press, New York, 1984) p. 151.
[9] X. Wenyang, L. Ruifeng, D. Tao and M. Jinghong, Zeolites 10 (1990) 200.
[10] E. Costa, M.A. Uguina, A. de Lucas and J. Blanes, J. Catal. 107 (1987) 317.
[11] W.F. Hillebrand, C.E.F. Lundell, H.H. Bright and J.I. Hoffman, *Applied Inorganic Analysis* (Wiley, New York, 1953).
[12] G. Calleja, A. de Lucas and R. van Grieken, Appl. Catal. 68 (1991) 11.
[13] D.Z. Wang, X.D. Lu, X.Y. Dou, W.B. Li and C.H. Yang, Appl. Catal. 59 (1990) 75.
[14] S.S. Pollack, J.W. Adkins, E.L. Wetzel and D. Newbury, Zeolites 4 (1984) 181.
[15] E.P. Parry, J. Catal. 2 (1963) 371.
[16] M.R. Basila and T.R. Kantner, J. Phys. Chem. 70 (1966) 1681.
[17] J.C. Vedrine, A. Auroux, V. Bolis, P. Dejaijve, C. Naccache, P. Wierchowski, E.G. Derouane, J.B. Nagy, J.P. Gilson, J.H.C. van Hooff, J.P. van den Berg and J. Wolthuizen, J. Catal. 69 (1979) 248.
[18] N.Y. Topsoe, K. Pedersen and E.G. Derouane, J. Catal. 70 (1981) 41.